The Accuracy of Multi-Slice Multi-Frequency MR Elastography in a Brain Stiffness Mimicking Phantom

Arvin Arani[1], Ondrej Slezak[1], Nikoo Fattahi[1], Kevin J Glaser[1], Joel Felmlee[1], Armando Manduca[2], Clifford R. Jack[1], Richard L. Ehman[1], and John Huston III[1]
[1]*Radiology, Mayo Clinic, Rochester, Minnesota, United States,* [2]*Physiology and Biomedical Engineering, Mayo Clinic, Rochester, Minnesota, United States*

Target audience: Neuroradiologists, neurologists, and physicists interested in the viscoelastic properties of the brain.

Purpose: Several groups have investigated the use of magnetic resonance elastography (MRE) in neurological diseases including brain tumors[1], normal pressure hydrocephalus[2] and Alzheimer's disease[3]. These studies have involved either using a single vibration frequency or the use of multi-frequency data to acquire information about the viscoelastic properties of brain tissues [2, 4-7]. Although the precision, repeatability, and sensitivity to changes in these viscoelastic parameters has been reported in phantoms[8] and *in vivo* [9], the accuracy of either the single-frequency or multi-frequency stiffness measurements has not been thoroughly evaluated experimentally. The objective of this work is to evaluate the accuracy of both single-frequency and multi-frequency brain MRE in a geometrically accurate brain stiffness mimicking phantom.

Methods: A brain phantom was made by pouring a polyvinyl chloride gel (PVC) into an anatomically correct plastic skull phantom (3B Scientific, USA). The PVC gel (plastic formula #502, Lure-craft, IN, USA) was composed of 50% PVC and 50% softener. Ice filled balloons attached to an acrylic rod were used to form and simulate the ventricles of the brain. Once the gel had set, the balloons were popped and removed while keeping the acrylic tube in place. The ventricles were then filled with water to simulate cerebral spinal fluid. Two cylindrical tube (9 mm inner diameter) samples were also filled with PVC from the same pour as the phantom and tested with a commercially available dynamic mechanical testing (DMA) machine (RheoSpectris^{TM} 400, QC, Canada) for stiffness comparison. The PVC brain phantom was placed on a clinically used pillow-type MRE passive driver and taped in place to an 8-channel MRI head coil. Image acquisition included a modified spin-echo echo planar imaging sequence to acquire MRE data with the following imaging parameters: 40-80Hz (step 10Hz) vibration; TR/TE = 3600/62 ms; FOV = 24 cm; 72x72 image matrix reconstructed to 80x80; 48 contiguous 3-mm-thick axial slices; one vibration frequency matched motion-encoding gradient on each side of the refocusing RF pulse; x, y, and z motion-encoding directions; and 8 phase offsets spaced evenly over one period of the vibration motion. MRE post-processing was performed in 3 steps: 1) calculating the curl of the displacement images; 2) calculating the stiffness using direct inversion of the Helmholtz wave equation, and 3) applying a 3x3x3 kernel median filter. To help reduce the effects of noise in our estimates the octahedral shear strain SNR (OSS SNR)[10] was calculated for each voxel, and voxels with OSS SNR less than 5 were not included in the stiffness calculations. For each vibration frequency the mean and median values of the storage shear modulus (G'), the loss shear modulus (G''), the magnitude of the complex shear modulus (|G*|), and the velocity squared (v^2) stiffness were calculated over the entire brain phantom volume. The percent error (100*(DMA-MRE)/DMA) between the DMA results and the MRE results were calculated for each stiffness measurement at each frequency. Lastly, the multi-frequency MRE and DMA data were fit to three viscoelastic models (Voigt, Maxwell, and a previously published springpot model [6]) and the percent error between the MRE and the DMA model parameter was calculated to estimate error propagation in these models.

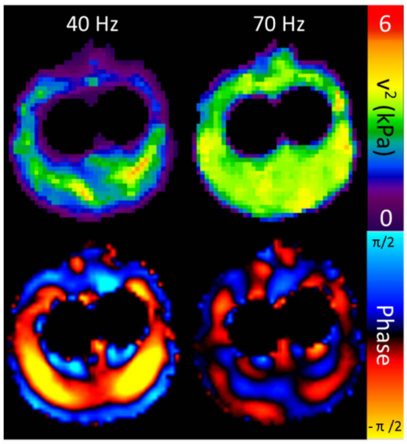

Figure 1: Sample elastograms (top row) and z-direction curl wave images (bottom row) at 40 Hz and 70 Hz.

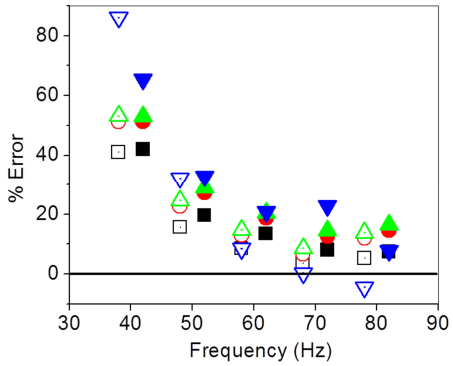

Figure 2: Percent error in v^2 (black square), |G*| (red circle), G' (green triangle), and G'' (blue triangle) between DMA and MRE as a function of vibration frequency. The mean values have been represented by solid filled shapes and the median has been represented by unfilled shapes.

		40-80Hz		60-80Hz	
Model	**Parameters**	**%Error Mean**	**%Error Median**	**%Error Mean**	**%Error Median**
Voigt	μ (kPa)	27	23	17	12
	η (kPa-s/rad)	24	14	19	4
Maxwell	μ (kPa)	27	23	17	12
	η (kPa-s/rad)	36	34	42	45
Springpot	$\kappa(kPa^{(1-\alpha)}*(kPa\text{-}s/rad)^{\alpha})$	33	31	20	19
	α	-33	-39	-13	-25

Table 1: Percent error in viscoelastic parameters over the 40-80Hz and the 60-80Hz range between DMA and MRE.

Results: The DMA samples reported v^2, |G*|, G', and G'' to be 3.32-3.42 kPa, 3.32-3.41 kPa, 3.38-3.46 kPa, and 0.21-0.33 kPa for the PVC phantom over the 40-80Hz frequency range, respectively. All DMA stiffness repeatability standard deviations were below 5% for all frequencies. Sample MRE wave images at 40 Hz and 70 Hz with corresponding elastograms are shown in Figure 1. The percent errors for all four stiffness measurements with respect to the corresponding DMA values have been plotted in Figure 2 for both mean (solid filled shapes) and median (open shapes) MRE stiffness measurements. Finally, the propagation of error introduced into commonly used viscoelastic models has been demonstrated over two ranges 40-80Hz (5 data points) and 60-80Hz (3 data points).

Discussion: Figures 1 and 2 demonstrate that increasing vibration frequencies significantly improves image quality and decreases the percent error in all stiffness measurements when using a standard direct inversion algorithm. Furthermore, Table 1 demonstrates that these errors propagate into viscoelastic parameter measurements, and can translate to parameter estimate errors on the order of 14-39%. However, if only higher frequencies are used, these errors are decreased, on the order of 2-3 fold for the Voigt and springpot model. The Maxwell model did not follow this behavior, but this model did not fit the DMA data well either, and may not be a suitable model for this specific phantom. It must be emphasized since no true gold standard exists for measuring the stiffness of soft tissues, these error estimates should be thought of more as experimental difference between MRE and DMA techniques and not the absolute error. However, it is encouraging that at higher frequencies, where MRE appears to produce the most uniform stiffness images the stiffness measurements of two techniques begin to converge. In conclusion, it is vital to ensure that the appropriate driving frequency range is determined before interpreting stiffness measurements and viscoelastic parameters even in a large organ like the brain. This work motivates future work in exploring the applications of higher driving frequencies in the brain. The methodology presented in this abstract could be a useful approach for experimentally validating different reconstruction algorithms, and understanding the mechanisms behind some of these reported errors.

References:

[1] Xu, L., et al., *Magnetic resonance elastography of brain tumors: preliminary results.* Acta Radiol, 2007. 48(3): p. 327-30. **[2]** Streitberger, K.J., et al., *In vivo viscoelastic properties of the brain in normal pressure hydrocephalus.* NMR Biomed, 2011. 24(4): p. 385-92. **[3]** Murphy, M.C., et al., *Decreased brain stiffness in Alzheimer's disease determined by magnetic resonance elastography.* J Magn Reson Imaging, 2011. 34(3): p. 494-8. **[4]** Zhang, J., et al., *Viscoelastic properties of human cerebellum using magnetic resonance elastography.* J Biomech, 2011. 44(10): p. 1909-13. **[5]** Streitberger, K.J., et al., *Brain viscoelasticity alteration in chronic-progressive multiple sclerosis.* PLoS One, 2012. 7(1): p. e29888. **[6]** Sack, I., et al., *The impact of aging and gender on brain viscoelasticity.* Neuroimage, 2009. 46(3): p. 652-7. **[7]** Murphy, M.C., et al., *Preoperative assessment of meningioma stiffness using magnetic resonance elastography.* J Neurosurg, 2013. 118(3): p. 643-8. **[8]** Guo, J., et al., *Fractal network dimension and viscoelastic powerlaw behavior: II. An experimental study of structure-mimicking phantoms by magnetic resonance elastography.* Phys Med Biol, 2012. 57(12): p. 4041-53. **[9]** Murphy, M.C., et al., *Measuring the characteristic topography of brain stiffness with magnetic resonance elastography.* PLoS One, 2013. 8(12): p. e81668. **[10]** McGarry, M.D., et al., *An octahedral shear strain-based measure of SNR for 3D MR elastography.* Phys Med Biol, 2011. 56(13): p. N153-64.